The Cooperative Control of tracking and vibration suppression of Flexible truss with Twin-Gyro Precession

Jin Qibao

June 27, 2020

The Cooperative Control of tracking and vibration suppression of Flexible truss with Twin-Gyro Precession

Qibao Jin[a,*]

[a] *School of Mechanical and Power Engineering, Guangdong Ocean University Zhanjiang, 524088, PR China*

[*] *Correspongding author. E-mail address*: qibaojin@gdou.edu.cn (Jin Q B)

***Abstract*—This paper presents a composite control approach which can track the desired trajectory and suppress vibration of a flexible truss undergoing a long-duration slewing motion. An improved PD state feedback master controller is proposed to implement such tasks as sinusoidal slewing tracking, which has advantages of wide dynamic range, high accuracy, fast response and little overshoot compared to the conventional PD controller. Moreover, an auxiliary direct modal force compensator is formulated to dissipate the vibration of flexible truss. With the composite strategy, the tracking performance can be further improved so that the whole system achieves the cooperative control. The simulation results demonstrate the validity and effectiveness of the combining control strategies.**

Keywords*—*Cooperative control; Active control; State feedback

I. INTRODUCTION

The control-moment-gyros(CMGs) have been used to exchange capacity either in attitude maneuver or slewing tracking (Ref. [1]). Reference [2] employed to suppress vibration suppress vibration of flexible spacecraft during attitude maneuver and a novel direct modal control strategy is exerted to elastic dynamics due to interaction between CMGs and flexibilities of structure. Reference [3] presents a generic global matrix formulation to deriving a minimum set of dynamic equations for robot system driven by skew-symmetric CMGs, based on which the vibration energy of flexible bodies are mitigated via the active gyroscopic torques. Reference [4] proposed a dynamic controller for a spacecraft with flexible appendages and ensures the asymptotic fulfillment of the objectives only in the case of rest-to-rest maneuver. Also, the above studies have no distinctly improvement in response rate and disturbance suppressing effectiveness. The paper [5] design a hybrid thruster/reaction wheel (RW) system to realize the active vibration suppression of a flexible spacecraft embedded with collocated and Non-collocated configuration of piezoelectric patches while it is unpractical for large-sized flexible control. However, all the existing methods in (Ref. [6-11]) employed angular rate sensors to measure the elastic rotational displace-ments at nodes where CMGs are mounted, whose accuracy can't be guaranteed because of the high-frequency vibration leading to unexpected disturbance. In this paper, a composite control scheme is proposed to achieve the cooperative control of the flexible system undergoing large-angle maneuvering motion driven by CMGs, especially, the improved PD state control designing enhances the tracking effectiveness. In this paper, The mechanical model of a large space flexible truss system is built and a new composite scheme is presented to implement attitude slewing tracking and solve the active vibration control problem by applying way to augment structural damping. The general schematic diagram is shown in Fig. 1.

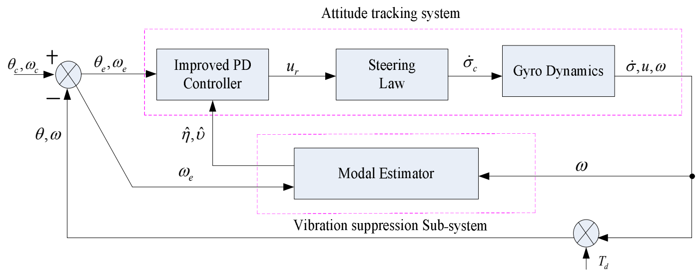

Fig. 1. Block diagram of slewing tracking dynamics system with vibration reduction.

II. CONTROLLER DESIGN

A. *Dynamics model of slewing system*

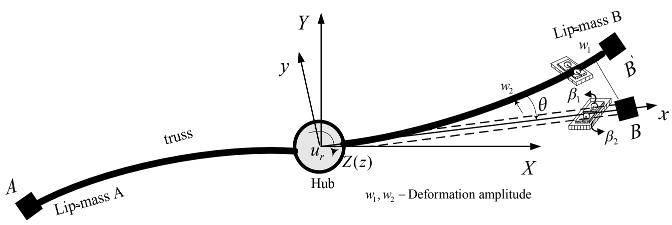

Fig. 2. CMG-Hub-truss slewing system.

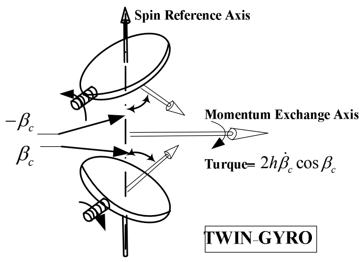

Fig.3. The momentum exchange axis with twin-gyro configuration.

In this section, the control mechanism are studied which couples together with flexible truss attached with lip masses shown in Fig. 2 with driving equipment in Fig.3 to implement the task of long-duration slewing around Z-axis, in this task, the stable slewing motion and the vibration suppression are both in consideration with the improved PD state controller.

Based on Newton-Euler dynamics theorem and hypothesis of small elastic deformations and the neglect of J_h, in the paper, the dynamics equation of the flexible spacecraft with V-gimbaled CMGs is formulated, which has the same mass as that (Ref. [12]) described by follows:

$$\mathbf{J}_b\dot{\boldsymbol{\omega}} + \boldsymbol{\delta}^T\ddot{\boldsymbol{\eta}} = -\tilde{\boldsymbol{\omega}}\left(\mathbf{J}_b\boldsymbol{\omega} + \mathbf{H}_h + \boldsymbol{\delta}^T\dot{\boldsymbol{\eta}}\right) - \mathbf{D}\dot{\boldsymbol{\sigma}} \tag{1}$$

$$\ddot{\boldsymbol{\eta}} + \mathbf{C}\dot{\boldsymbol{\eta}} + \mathbf{K}\boldsymbol{\eta} = -\boldsymbol{\delta}\dot{\boldsymbol{\omega}} \tag{2}$$

where J_b is the symmetric inertia matrix of the flexible truss main body, $\boldsymbol{\delta}$ is the coupling matrix between the central rigid hub and flexible truss system, $\boldsymbol{\eta}$ is the modal coordinate vector; $\mathbf{H}_c = \sum_{i=1}^{N}\mathbf{C}_i^T\left(\mathbf{J}_h\mathbf{C}_i\boldsymbol{\omega} + \mathbf{J}_h\dot{\boldsymbol{\sigma}}_i + \mathbf{h}\right)$ denotes the total angular momentum relating to the frames and gyros, where $\mathbf{C}_i$ is i th matrix for coordinate transform from gimbal frame to body frame, $\mathbf{J}_h$ is the inertia matrix of each gyro, $\dot{\boldsymbol{\beta}}_i$ represents the gimbal angular velocity vector of the i th CMG, and $\mathbf{h}$ is defined as the output of angular momentum of each gyro. $\boldsymbol{\omega}$ is in the body coordinate system $o-xyz$ and $\tilde{\boldsymbol{\omega}}$ denotes the cross product array. $C = diag\left[2\varsigma_i\omega_{ni},\ i=1,\ \cdots\ N\right]$ and $K = diag\left[\omega_{ni}^2,\ i=1,\ \cdots\ N\right]$ are the damping and stiffness matrices, respectively, where ω_{ni} and ς_i are the natural frequency and related damping of the i th mode. In Eq. (1-1), $\mathbf{D}\dot{\boldsymbol{\sigma}}$ is the total output torque of the CMG array which is expressed by the new variable

$$L_c = \mathbf{D}\dot{\boldsymbol{\sigma}} \tag{3}$$

and another new variable $\boldsymbol{\upsilon} = \boldsymbol{\delta}\boldsymbol{\omega} + \dot{\boldsymbol{\eta}}$ for the total velocities of the flexible truss, and finally, the dynamic equation can be thereby written as

$$\dot{\boldsymbol{\omega}} = -\mathbf{J}_m^{-1}\left[\tilde{\boldsymbol{\omega}}\left(\mathbf{J}_b\boldsymbol{\omega} + \mathbf{H}_h + \boldsymbol{\delta}^T\dot{\boldsymbol{\eta}}\right) - \boldsymbol{\delta}^T\left(\mathbf{C}\boldsymbol{\upsilon} + \mathbf{K}\boldsymbol{\eta} - \mathbf{C}\boldsymbol{\delta}\boldsymbol{\omega}\right) + \mathbf{D}_1\dot{\boldsymbol{\sigma}} - \mathbf{L}_e\right] \tag{4a}$$

$$\dot{\boldsymbol{\eta}} = \boldsymbol{\upsilon} - \boldsymbol{\delta}\boldsymbol{\omega} \tag{4b}$$

$$\dot{\boldsymbol{\upsilon}} = -\mathbf{C}\boldsymbol{\upsilon} - \mathbf{K}\boldsymbol{\eta} + \mathbf{C}\boldsymbol{\delta}\boldsymbol{\omega} \tag{4c}$$

where $\mathbf{J}_m = \mathbf{J}_b - \boldsymbol{\delta}^T\boldsymbol{\delta}$ and $\mathbf{L}_e$ denotes the constant disturbance on the hub-truss body.

B. Improved state feedback controller for slewing

To steer the overall truss arm slewing motion by twin-gyro synchronization precession, a output feedback controller is designed; Meanwhile, considering the vibration excited by the rapid maneuver or tracking, a companion feedback controller is employed to avoid chattering for maneuver and suppress the relatively large amplitude vibrations for continuous trajectory tracking. Specially when Euler angles is chosen as parameters describing the truss attitude, the overall slewing

In light of the dynamic Eq. (4a) -Eq. (4c), assuming that the slewing axis is $z-axis$, slewing angle vector $\boldsymbol{\theta}$ are now measurable, and desired angle vector $\boldsymbol{\theta}_c$, tracking error $\mathbf{e}_1 = \boldsymbol{\theta} - \boldsymbol{\theta}_c$ and velocity error $\mathbf{e}_2 = \boldsymbol{\omega} - \boldsymbol{\omega}_c$, where $\boldsymbol{\theta}_c$ and $\boldsymbol{\omega}_c$ are known. If $\mathbf{e}_{\boldsymbol{\eta}} = \boldsymbol{\eta} - \hat{\boldsymbol{\eta}}$ and $\mathbf{e}_{\boldsymbol{\upsilon}} = \boldsymbol{\upsilon} - \hat{\boldsymbol{\upsilon}}$ are defined as estimate error of modal and velocity, respectively; meanwhile, the modal variables η, ν are supposed unmeasurable. Base the traditional PD controller (Ref. [13]), the following improved dynamic control law is sufficient to ensure the global asymptotic stability:

$$\mathbf{u}_r = \left[k_p\mathbf{I}, \delta^T\left\{\begin{bmatrix}K\\C\end{bmatrix} - P_1\begin{bmatrix}I\\-C\end{bmatrix}\right\}^T\right]\begin{bmatrix}\boldsymbol{\theta}\\\hat{\eta}\\\hat{\upsilon}\end{bmatrix} - J_m\dot{\boldsymbol{\omega}}_c - \boldsymbol{\omega}\times\left(J_b\boldsymbol{\omega} + H_h + \delta^T\dot{\eta}\right)$$
$$-k_p\boldsymbol{\theta}_c - \delta^T C\delta\boldsymbol{\omega} + k_d(\boldsymbol{\omega} - \boldsymbol{\omega}_c) \tag{5}$$

and auxiliary suppressing vibration controller

$$\begin{bmatrix}\dot{\hat{\eta}}\\\dot{\hat{\upsilon}}\end{bmatrix} = \begin{bmatrix}0 & I\\-K & -C\end{bmatrix}\begin{bmatrix}\hat{\eta}\\\hat{\upsilon}\end{bmatrix} - \begin{bmatrix}I\\-C\end{bmatrix}\delta\boldsymbol{\omega} + P_2^{-1}\begin{bmatrix}K\\C\end{bmatrix}\delta(\boldsymbol{\omega} - \boldsymbol{\omega}_c) - P_2^{-1}P_1\begin{bmatrix}I\\-C\end{bmatrix}\delta\boldsymbol{\omega} \tag{6}$$

where $\boldsymbol{\theta}$ and $\boldsymbol{\omega}$ are assumed measurable and as feedback parameters, $\mathbf{I}$ is 2×2 identity matrix and k_p、k_d are positive constants, $\mathbf{P}_i = \mathbf{P}_i^T (i=1,2)$ are symmetric positive-definite matrices. Choose the candidate Lyapunov function

$$V = \frac{1}{2}k_p\mathbf{e}_1^T\mathbf{e}_1 + \frac{1}{2}\mathbf{e}_2^T J_m\mathbf{e}_2 + \frac{1}{2}\begin{bmatrix}\eta^T & \upsilon^T\end{bmatrix}P_1\begin{bmatrix}\eta\\\upsilon\end{bmatrix} + \frac{1}{2}\begin{bmatrix}\mathbf{e}_\eta^T & \mathbf{e}_\upsilon^T\end{bmatrix}P_2\begin{bmatrix}\mathbf{e}_\eta\\\mathbf{e}_\upsilon\end{bmatrix} \tag{7}$$

The derivative of the Lyapunov Eq. (7) is then expressed by

$$\dot{V} = k_p\dot{\mathbf{e}}_1^T\mathbf{e}_1 + \mathbf{e}_2^T J_m\dot{\mathbf{e}}_2 + \begin{bmatrix}\eta^T & \upsilon^T\end{bmatrix}P_1\begin{bmatrix}\dot{\eta}\\\dot{\upsilon}\end{bmatrix} + \begin{bmatrix}\mathbf{e}_\eta^T & \mathbf{e}_\upsilon^T\end{bmatrix}P_2\begin{bmatrix}\dot{\mathbf{e}}_\eta\\\dot{\mathbf{e}}_\upsilon\end{bmatrix} \tag{8}$$

For the first two terms in Eq. (8)

$$\begin{aligned}
&k_p\dot{\mathbf{e}}_1^T\mathbf{e}_1 + \mathbf{e}_2^T J_m\dot{\mathbf{e}}_2\\
&= k_p(\boldsymbol{\omega}^T - \boldsymbol{\omega}_c^T)(\boldsymbol{\theta} - \boldsymbol{\theta}_c) + (\boldsymbol{\omega}^T - \boldsymbol{\omega}_c^T)J_m(\dot{\boldsymbol{\omega}} - \dot{\boldsymbol{\omega}}_c)\\
&= -(\boldsymbol{\omega}^T - \boldsymbol{\omega}_c^T)\left[J_m(\dot{\boldsymbol{\omega}}_c - \dot{\boldsymbol{\omega}}) - k_p(\boldsymbol{\theta} - \boldsymbol{\theta}_c)\right]\\
&= -(\boldsymbol{\omega}^T - \boldsymbol{\omega}_c^T)[J_m\dot{\boldsymbol{\omega}}_c + \boldsymbol{\omega}\times\left(J_b\boldsymbol{\omega} + H_h + \delta^T\dot{\eta}\right)\\
&\quad -\delta^T\left(C\upsilon + K\eta - C\delta\boldsymbol{\omega}\right) + \mathbf{u}_r - k_p(\boldsymbol{\theta} - \boldsymbol{\theta}_c)]
\end{aligned} \tag{9}$$

Substituting Eq. (9) into Eq. (8), and considering Eq. (5) and Eq. (6), the Eq. (8) is now transformed into

$$\begin{aligned}
\dot{V} &= -(\boldsymbol{\omega}^T - \boldsymbol{\omega}_c^T)\left[J_m\dot{\boldsymbol{\omega}}_c + \boldsymbol{\omega}\times\left(J_b\boldsymbol{\omega} + H_h + \delta^T\dot{\eta}\right) - \delta^T\left(C\upsilon + K\eta - C\delta\boldsymbol{\omega}\right) + \mathbf{u}_r - k_p(\boldsymbol{\theta} - \boldsymbol{\theta}_c)\right]\\
&\quad + \begin{bmatrix}\eta^T & \upsilon^T\end{bmatrix}P_1\begin{bmatrix}\dot{\eta}\\\dot{\upsilon}\end{bmatrix} + \begin{bmatrix}\mathbf{e}_\eta^T & \mathbf{e}_\upsilon^T\end{bmatrix}P_2\begin{bmatrix}\dot{\mathbf{e}}_\eta\\\dot{\mathbf{e}}_\upsilon\end{bmatrix}\\
&= -(\boldsymbol{\omega}^T - \boldsymbol{\omega}_c^T)[J_m\dot{\boldsymbol{\omega}}_c + \boldsymbol{\omega}\times\left(J_b\boldsymbol{\omega} + H_h + \delta^T\dot{\eta}\right) - \delta^T\left(C\upsilon + K\eta - C\delta\boldsymbol{\omega}\right) - \delta^T C\delta\boldsymbol{\omega} +\\
&\quad \left[k_p, \delta^T\left\{\begin{bmatrix}K\\C\end{bmatrix} - P_1\begin{bmatrix}I\\-C\end{bmatrix}\right\}^T\right]\begin{bmatrix}\boldsymbol{\theta}\\\hat{\eta}\\\hat{\upsilon}\end{bmatrix} - J_m\dot{\boldsymbol{\omega}}_c - \boldsymbol{\omega}\times\left(J_b\boldsymbol{\omega} + H_h + \delta^T\dot{\eta}\right) - k_p\boldsymbol{\theta}_c +\\
&\quad k_d(\boldsymbol{\omega} - \boldsymbol{\omega}_c) - k_p(\boldsymbol{\theta} - \boldsymbol{\theta}_c)] + \begin{bmatrix}\eta^T & \upsilon^T\end{bmatrix}P_1\left\{\begin{bmatrix}0 & I\\-K & -C\end{bmatrix}\begin{bmatrix}\eta\\\upsilon\end{bmatrix} - \begin{bmatrix}I\\-C\end{bmatrix}\delta\boldsymbol{\omega}\right\} +\\
&\quad \begin{bmatrix}\mathbf{e}_\eta^T & \mathbf{e}_\upsilon^T\end{bmatrix}P_2\left\{\begin{bmatrix}0 & I\\-K & -C\end{bmatrix}\begin{bmatrix}\eta\\\upsilon\end{bmatrix} - \begin{bmatrix}I\\-C\end{bmatrix}\delta\boldsymbol{\omega} - \begin{bmatrix}0 & I\\-K & -C\end{bmatrix}\begin{bmatrix}\hat{\eta}\\\hat{\upsilon}\end{bmatrix} +\right.\\
&\quad \left.\begin{bmatrix}I\\-C\end{bmatrix}\delta\boldsymbol{\omega} - P_2^{-1}\begin{bmatrix}K\\C\end{bmatrix}\delta(\boldsymbol{\omega} - \boldsymbol{\omega}_c) + P_2^{-1}P_1\begin{bmatrix}I\\-C\end{bmatrix}\delta\boldsymbol{\omega}\right\}
\end{aligned} \tag{10}$$

Letting $\mathbf{P}_i$ is the solution of the following Lyapunov equation

$$P_i\begin{bmatrix}0 & I\\ -K & -C\end{bmatrix}+\begin{bmatrix}0 & I\\ -K & -C\end{bmatrix}^T P_i=-2Q_i,\quad i=1,2 \tag{11}$$

where $Q_i=Q_i^T(i=1,2)$ are symmetric positive-definite matrices.The Lyapunov function is ultimately obtained by

$$\begin{aligned}\dot{V}&=-(\boldsymbol{\omega}^T-\boldsymbol{\omega}_c{}^T)k_d(\boldsymbol{\omega}-\boldsymbol{\omega}_c)\\&-\begin{bmatrix}\eta^T & \upsilon^T\end{bmatrix}Q_1\begin{bmatrix}\eta\\ \upsilon\end{bmatrix}-\begin{bmatrix}\mathbf{e}_\eta{}^T & \mathbf{e}_\upsilon{}^T\end{bmatrix}Q_2\begin{bmatrix}\mathbf{e}_\eta\\ \mathbf{e}_\upsilon\end{bmatrix}<0\end{aligned} \tag{12}$$

According to the LaSalle invariance principle (Ref. [14]), the control system in following two slewing mode respectively results in:

A. Rest-to-rest maneuver slewing

$\boldsymbol{\omega}\to\boldsymbol{\omega}_c\to 0$, $\boldsymbol{\theta}-\boldsymbol{\theta}_c\to 0$, $\boldsymbol{\eta}\to 0$, $\boldsymbol{\upsilon}\to 0$, $\boldsymbol{\eta}\to\hat{\boldsymbol{\eta}}$ and $\boldsymbol{\upsilon}\to\hat{\boldsymbol{\upsilon}}$, tracking **error** of slew angle $\boldsymbol{\theta}-\boldsymbol{\theta}_c$ converges to zero along the trajectories of the controlled system $\dot{\boldsymbol{\omega}}=-\mathbf{J}_m^{-1}\left[\mathbf{0}+k_p\left(\boldsymbol{\theta}-\boldsymbol{\theta}_c\right)\right]=0$ as $t\to\infty$;

B. Sinusoidal tracking slewing

Similar to mode (I), since $\boldsymbol{\theta}\to\boldsymbol{\theta}_c$, $\|\boldsymbol{\theta}-\boldsymbol{\theta}_c\|<\delta$, where δ is a maximum boundary value, the tracking error of slew angle $\boldsymbol{\theta}-\boldsymbol{\theta}_c$ is bounded and takes cyclic variation along the system $\dot{\boldsymbol{\omega}}=-\mathbf{J}_m^{-1}\left[\mathbf{0}+k_p\left(\boldsymbol{\theta}-\boldsymbol{\theta}_c\right)\right]=-k_p\mathbf{J}_m^{-1}\left(\boldsymbol{\theta}-\boldsymbol{\theta}_c\right)$ as $t\to\infty$.

III. Simulation Results and Discussion

The parameters of the hub-truss system installed with gimbaled CMGs are listed in Table 1:

TABLE I. MODEL PARAMETERS OF CMG-HUB-TRUSS SYSTEM

Hub	Radius/m	$R=60$
	Density/kg/m³	$\rho=2766.67$
Lip Mass	Weight(Kg)	$M=4\times10^4$
Truss	Length/m	$l=600$
	Cross section/ m²	$A=24$
	Elastic modulus	$E=68.944$Gpa
Gyro	Limit gimbal angle/ °	$\beta_{\max}=90^\circ$
	Angular momentum, kg.m²/s	$h=4.5\times10^3$
	Moment of gimbal, kg.m²/s	$J_g=3\times10^4$

The CMG-hub-truss consists of a rigid hub and a flexible truss with a pairs of V-gimbal CMGs, beside above parameters, the coupling matrix is $\delta=$[10 10 10; 0.5 2 0; 0.1 10.9 0.8; 1 0.5 0.5]; For the flexible truss, the natural frequencies of the first four modes and associated damping are given as $\omega_{n1}=1.9$, $\omega_{n2}=4.1$, $\omega_{n3}=5.8$, $\omega_{n4}=6$; $\zeta_1=0.05$, $\zeta_2=0.04$, $\zeta_3=0.16$, $\zeta_4=0.005$ .The initial gimbal angles of gyros and their rates are zero. The whole large-angle slewing mission is discussed with the following rest-to-rest maneuver slewing.

In this slew task, the parameters of the slewing controller are selected as $k_p=13$, $k_d=250$, $Q_1=I$, $Q_2=2.5I$, the CMGs controller, weighting matrices are chosen as $R=diag\left(1\quad 1\right)$, $Q=\left[10^6\quad 10^3\quad 10^3\quad 10^2\quad 10^2\right]$, the synchronous controller for twin-gyro is parameterized by $c_1=c_2=c_3=c_4=10$. In the whole slewing task, constant disturbances $d=\left[0.3\quad -0.1\right]^T$ are imposed on the gimbal axes of the CMGs system, the initial disturbances imposed is $\hat{d}(0)=\left[0\quad 0\right]^T$. The range of gimbal angle and angular rate are both restrained to prevent singularity occurred in the task: $\beta_{1,2\max}\le\pi/2$, $\dot{\sigma}_{1,2\max}\le 0.5$; the slewing starts from $\dot{\theta}(0)=0^\circ$ /s without taking the external disturbance into account, the large-angle slewing mission rest-to-rest 90° slewing is shown as Fig.3,

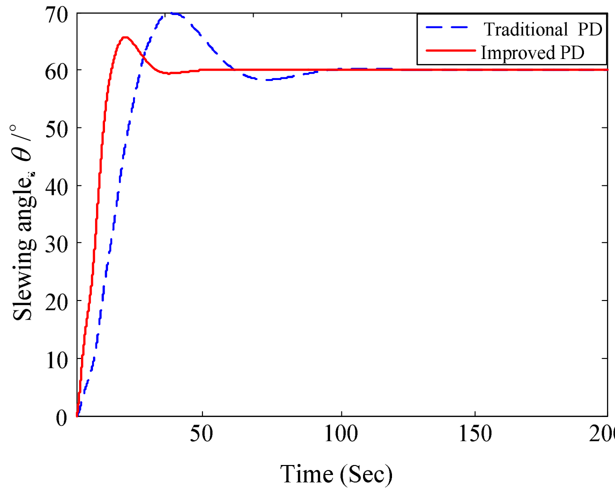

(a) The maneuver tracking error comparison of different PD algorithm

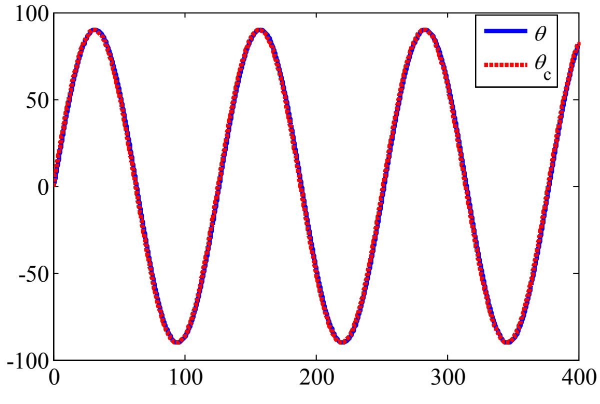

(b) The sinusoidal tracking error comparison of improved PD algorithm

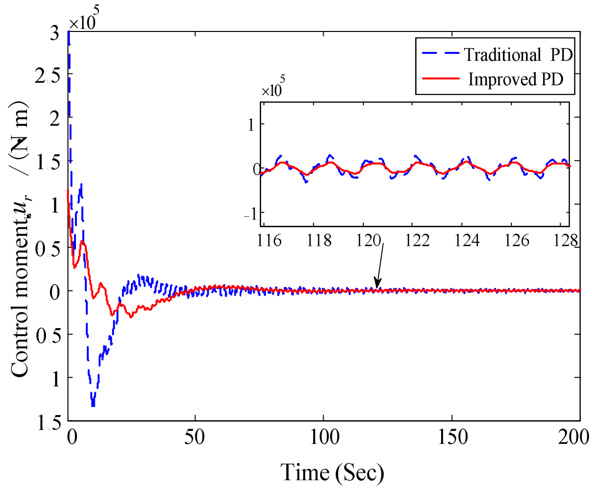

(c) The output control moments comparison of different PD algorithm

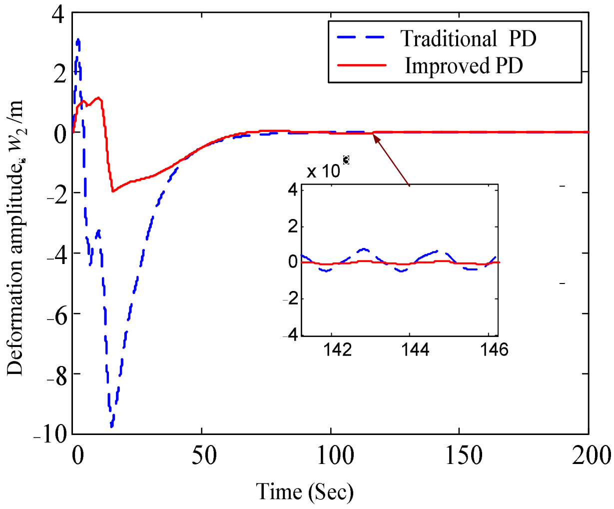

(d) The deformation amplitude of w_1 comparison comparison of different PD algorithm

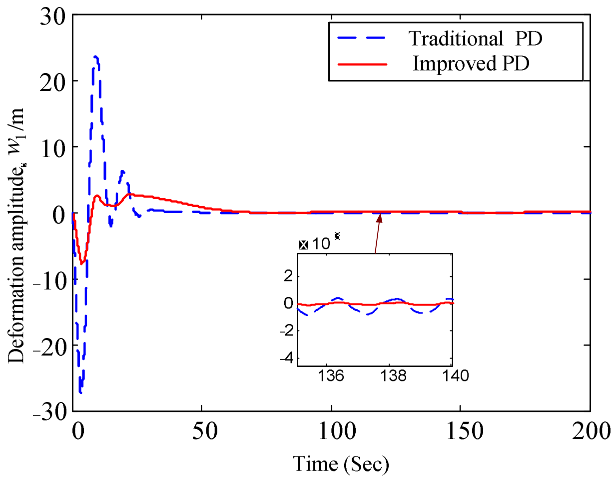

(e) The deformation amplitude of w_1 comparison comparison of different PD algorithm

Fig. 4. Maneuver slewing and twin-gyro synchronization precession.

The simulation parameters of the both controller are chosen to be the same as in Table1. In the master controller scheme as shown in Fig. 3a, both master controllers can smoothly perform the maneuver task, the vibration deflections can be well suppressed within a maximum of 70 sec and the residual oscillations are gradually attenuated to zero, the proposed controller has a faster response speed and more stable precision than does the traditional PD in the maneuver slewing task, and the former outputs smaller output amplitude than does the latter. Obviously, the improved PD controller achieves more preferable performance than traditional one. Further, The output from the traditional PD controller converges to zero long before the improved one. Fig. 4b shows the gyros control moment of the improved are more effective than that of the latter. In vibration suppression, the traditional scheme can ultimately suppress deflection but respond slowly; in contrast to the former, the improved scheme can rapidly suppress vibration within 25 seconds (Fig. 4c~Fig. 4d) while effectively tracking the position of the tip deflection of the flexible beam according to the desired trajectory. The synchronization precession of the twin-gyro are plotted in Fig. 4e and Fig. 4f which illustrates two gyros are perfect synchronal and coincide with each other, respectively, thus he performance of the system using the proposed composite scheme is further improved.

IV. Conclusions

In this paper, a new approach for both maneuver slewing and tracking slewing of flexible truss actuated by twin-gyro is presented. Based on Newton-Euler dynamics and the principle of angular momentum exchange, the slewing dynamics model is derived. Assuming that the slew angle and command angle are measurable and as output feedback variables, a new output feedback controller is proposed according to the second method of Lyapunov, this control strategy guarantee the implementation of the large-angle single axis rotation in two modes: maneuver and tracking, and the tracking error asymptotically tracks its command. Beside that, an adaptive feedback nonlinear controller is designed to eliminate or suppress the vibration of the flexible truss in maneuver and tracking modes, respectively. The two combining control strategy greatly improve the stability performance of slewing motion.

V. Acknowledgments

This research is supported by Scientific Research Start-up fund project from the Guangdong Ocean University under Grant (No.R19054), Science and Technology Research project from Zhanjiang Science and Technology Bureau under Grant (No.2019B01155).

References

[1] Heiberg, C. J., Bailey, D., and Wie, B., Precision Spacecraft Pointing Using Single-Gimbal Control Moment Gyros With Disturbance, J. Guid. Con-trol Dyn., 2000, 23(1):77–85.

[2] Jitang Guo, Yunhai Geng, Baolin Wu, Xianren Kong. Vibration suppression flexible spacecraft during attitude maneuver using CMGs, Aerospace Science and Technology. 2018: 183-192.

[3] Xiao Feng, Yinghong Jia, Shijie Xu. Dynamics of flexible multibody systems with variable-speed control moment gyroscopes, Aerospace Science and Technology. 2018(79) :554-569.

[4] S.Di Gennaro, JOURNAL OF OPTIMIZATION THEORY AND APPLICATIONS: 2013,116(1):41–60.

[5] Azimi Milad, Sharifi Ghasem, A Hybrid Control Scheme for Attitude and Vibration Suppression of a Flexible Spacecraft using Energy-Based Actuators Switching, Aerospace Science and Technology. Volumes 82–83, November 2018, Pages 140-148.

[6] Di Gennaro, S., Passive Attitude Control of Flexible Spacecraft From Quaternion Measurements, J. Optim. Theory Appl., 2013, 116 (1), pp. 41–60

[7] Jixiang Fan, Di Zhou Nonlinear Attitude Control of Flexible Spacecraft With Scissored Pairs of Control Moment Gyros. Journal of Dynamic Systems, Measurement, and Control. 2017(34): 054502-1.

[8] S. di Gennaro, Active Vibration Suppression in Flexible Spacecraft Attitude Tracking, Journal of Guidance Control & Dynamics. 1998, 21(3):400-408.

[9] Wie, B., Singularity Analysis and Visualization for Single-Gimbal Con-trol Moment Gyro Systems, J. Guid. Control Dyn., 2004, 27(2): 271–282.

[10] Yang, L. F., Mikulas, M. M., Jr., Park, K. C., and Su, R., Slewing Maneuvers and Vibration Control of Space Structures by Feedforward/ Feedback Moment-Gyro Controls, ASME J. Dyn. Syst., Meas., Control, 1995,117(3):343–351.

[11] Greensite, A. L., 1970, (Control Theory: Volume II) Analysis and Design of Space Vehicle Flight Control Systems, Spartan Books, New York, NY.

[12] Jixiang Fan, Di Zhou Nonlinear Attitude Control of Flexible Spacecraft With Scissored Pairs of Control Moment Gyros. Journal of Dynamic Systems, Measurement, and Control. September 2012(134):054502-1.

[13] S. di Gennaro, Active Vibration Suppression in Flexible Spacecraft Attitude Tracking, Journal of Guidance Control & Dynamics. 1998, 21(3):400-408.

[14] Wie, B., 2004, “Singularity Analysis and Visualization for Single-Gimbal Con-trol Moment Gyro Systems,” J. Guid. Control Dyn. , 27(2): 271–282.